

## Article

# Study on Hydrochemical Characteristics and Formation Process of Antu Mineral Water in Changbai Mountain, China

Jianmin Bian <sup>1,2,3</sup>, Yihan Li <sup>1,2,3</sup>, Yuxi Ma <sup>1,2,3,4,\*</sup>, Jialin Li <sup>1,2,3</sup>, Yexiang Yu <sup>1,2,3</sup> and Wenhao Sun <sup>1,2,3</sup>

<sup>1</sup> Key Laboratory of Groundwater Resources and Environment, Ministry of Education, Jilin University, Changchun 130021, China

<sup>2</sup> College of New Energy and Environment, Jilin University, Changchun 130021, China

<sup>3</sup> Jilin Provincial Key Laboratory of Water Resources and Environment, Jilin University, Changchun 130021, China

<sup>4</sup> Organization Department of Yuyang District Committee, Yulin 719000, China

\* Correspondence: yxma\_cumt@126.com

**Abstract:** Changbai Mountain is the source region of the Songhua, Tumen, and Yalu Rivers. It is a famous concentrated distribution area of high-quality mineral water in China, which has a great economic value. Antu County is one of the main distribution areas of basalt and mineral water in Changbai Mountain. The distribution of mineral water has a strong hydraulic relationship with surface water, which constitutes abundant recharge reserves. It is important to study the hydrochemical characteristics and the relationship between surface water and mineral water to provide a theoretical basis for further discussion on the formation process and rational utilization of mineral water resources in Changbai Mountain. A total of 18 water samples in the period of abundant and dry water were collected, including rainwater, mineral water, and surface water. Geostatistics was utilized to analyze the hydrochemical characteristics. Hydrochemical component tracing and stable environmental isotope technology with end-number calculation reveals the transformation relationship between mineral and surface water. The results indicate that: (1) The hydrochemical type is mainly HCO<sub>3</sub>-Ca-Na and HCO<sub>3</sub>-Ca-Mg type. The average content of H<sub>2</sub>SiO<sub>3</sub> is 50.78 mg/L, which reach the standard of high quality metasilicate mineral water. (2) The mineral water formation process is dominated by the water-rock interaction in silicate mineral weathering. Metasilicate came from hydrolytic reaction of silicate and aluminosilicate under acidic conditions. (3) Atmospheric precipitation is the main recharge source, and the recharge area locates in the south nature reserve of the study area. The average retention time of mineral water is 35.5 years, and the recharge ratio of mineral water to surface water is up to 83.7%. This study will provide a theory guide for the protection and rational utilization of groundwater resources in study area and a reference for mineral spring formation study in basalt mountain area.

**Keywords:** Changbai Mountain; natural mineral water; hydrochemistry; isotopes; formation process



**Citation:** Bian, J.; Li, Y.; Ma, Y.; Li, J.; Yu, Y.; Sun, W. Study on Hydrochemical Characteristics and Formation Process of Antu Mineral Water in Changbai Mountain, China. *Water* **2022**, *14*, 2770. <https://doi.org/10.3390/w14182770>

Academic Editor: Cesar Andrade

Received: 6 August 2022

Accepted: 2 September 2022

Published: 6 September 2022

**Publisher's Note:** MDPI stays neutral with regard to jurisdictional claims in published maps and institutional affiliations.



**Copyright:** © 2022 by the authors. Licensee MDPI, Basel, Switzerland. This article is an open access article distributed under the terms and conditions of the Creative Commons Attribution (CC BY) license (<https://creativecommons.org/licenses/by/4.0/>).

## 1. Introduction

Groundwater is an essential natural and strategic resource, and plays an important role in the ecological environment system. It is also the material basis for human life and social development [1–5]. Among many types of groundwater resources, the role of mineral water cannot be ignored. Mineral water is not only beneficial for human health, but also helps to maintain natural ecological environment [6]. Therefore, studying the chemical composition and formation process of mineral water is the basis of rational utilization and protection of regional groundwater resources.

At present, the combination of hydrochemistry and stable isotope technology has been widely applied in the formation process and hydrologic cycle [7–15]. The most commonly used isotope in current research is hydrogen (D) and oxygen (<sup>18</sup>O) isotopes. They are

components of water molecules, so they can represent specific environments and reaction processes with tiny differences in mass.

The water cycle and amount of water resources discharged by groundwater runoff can be obtained by using environmental isotopes in the study area or specific hydrogeological units. Hydrochemistry data is a reflection of the results of the water-rock action process, while the solute also changes with water quantity exchange [16]. The chemical composition of natural water records the history of water formation and transport to a certain extent [17]. In addition, on the basis of the tracer method of conservative water chemistry and the principle of isotope mass conservation, the exchange relationship between different water bodies can be revealed. The formation mechanism of water and the interaction between groundwater and surface water have made remarkable achievements by using hydrochemistry and isotope method [18–26].

Changbai Mountain is one of the three high-quality water sources in the world [27,28]. The great storage conditions and abundant rainwater provide conditions for the formation of high-quality water resources. Mineral water resources are mainly distributed in Jingyu, Fusong, and Antu counties. There have been numerous researches on mineral water in Changbai Mountain Area. The researches focused on the distribution characteristics, formation conditions and sustainable utilization of mineral water in Jingyu and Fusong [27–40]. Compared with Jingyu and Fusong, the mineral water in Antu has a higher average content of metasilicate. However, the development and utilization of Antu mineral water is later than the other two areas, so there are few relevant studies.

In recent years, the mineral water industry is gradually developing into the pillar industry of Antu County, and the development degrees and utilization of mineral water are constantly improving, showing an explosive development trend from 2013 (Figure 1). From 2012 to 2019, the number of enterprises put into production increased from 2 to 10; the annual production capacity increased from 150,000 tons to 5 million tons; the annual production increased from 7000 tons to 2 million tons; the output value increased from 8 million yuan to 2.1 billion yuan. However, at present, the consumption of mineral water only accounts for 3.11%, staying at the level of resource consumption without deep utilization. In order to change the existing primary development and utilization of mineral water resources and further enhance its economic value and better maintain a virtuous cycle of ecology and environment, it is necessary to clarify chemical characteristics and formation process of mineral water.

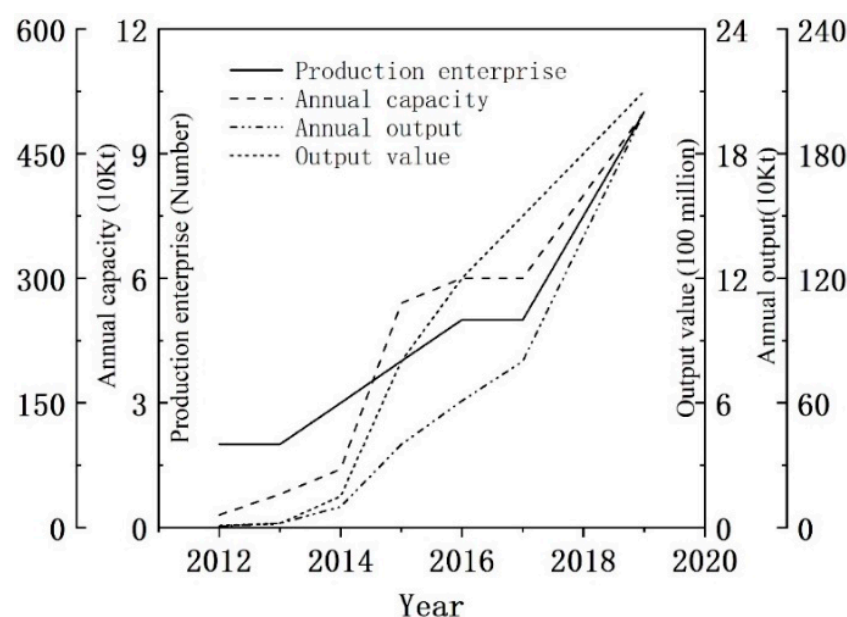


Figure 1. Development and utilization of mineral water resources in Antu county.

Based on this, the main research objectives of this paper are as follows: (1) clarify the spatial distribution characteristics of hydrochemistry and stable isotope of mineral water in Changbai Mountain and reveal the formation process of mineral water; (2) describe the influencing factors and reveal the mutual transformation relationship between mineral water and surface water. The results will help to promote effective utilization and to ensure the ecological security of Changbai Mountain.

## 2. Materials and Methods

### 2.1. Study Area

Antu County is located in the southeast of Jilin Province ( $127^{\circ}48'$ – $129^{\circ}08'$  E,  $42^{\circ}01'$ – $43^{\circ}24'$  N), at the north foot of Changbai Mountain. It belongs to the Yanbian Korean Autonomous Prefecture, with a total area of about 7400 km<sup>2</sup>. The average annual temperature is 4.0°C. The mean annual precipitation is 691.7 mm, with a decreasing trend from south to north. Precipitation mostly concentrates in June to August, accounting for 60% of the annual precipitation. The surface water belongs to Songhua River system. It is originated from Changbai Mountain and arranged in parallel from west to East. The Sandaobai River Basin is the concentrated distribution area of mineral water with a total length of 96.7 km and a channel ratio of 6.8‰.

The terrain is high in the south and low in the north, showing a stepped platform. Its highest point is located near Huangsongpu Forest Farm with a 1308 m elevation, and its lowest point is located north of Hongfeng Spring in the north with a 685-m elevation. Under the influence of multistage tectonics, the geological structures in the area are complex. The Xinghua–Baitou Mountain Tianchi fault zone is mainly developed in this area. Furthermore, the topography is composed mainly of an erosional volcanic lava mountain platform, erosional tectonic mountain, intermountain denudation basin, and intermountain valley plain. The main strata comprise the Neozoic Quaternary Lower Pleistocene System, and the covered rocks are the lava rocks of the Junjian mountain group ( $\beta Q_1$ ). The strata exposed in Antu are mainly Cenozoic volcanic rocks. The lithology is dominated by compact massive olivine basalt, stomatal basalt, and trachyte. The content of amorphous silica is high, which laid a material foundation for the formation of mineral water. Under the influence of volcanic activities, the faulted structure in the study area is developed. The groundwater type in the area is complete, including clastic rock fracture–pore water, carbonate fissure–cavern water, basalt pore fissure water, loose rock pore water, and bedrock fissure water. The basalt pore fissure water distribution is widespread and is closely related to the occurrence and formation of mineral springs with clastic rock fracture–pore water. The primary pore and structural fractures formed by condensation and contraction of magma after erupting to the surface are interlinked, providing a space for the lixiviation and migration of mineral water. Moreover, the study area had abundant rainwater and high vegetation coverage, which provide material source and conservation for mineral water.

### 2.2. Sample Collection and Testing

According to the Water Quality Sampling Technical Guide (HJ 494-2009), we collected water samples along the groundwater flow in April and September 2019. The area is full of typical springs, 17 representative points were selected for sample collection, including springs and river (Figure 2). A total of 15 hydrochemistry samples and 19 stable isotope samples were collected, including 14 natural outcrop spring samples and 1 surface water sample. Polyethylene bottles (500 mL) were used to collect water samples. Subsequently, the bottles were sealed, stored at 4 °C, and transported to the laboratory for testing.

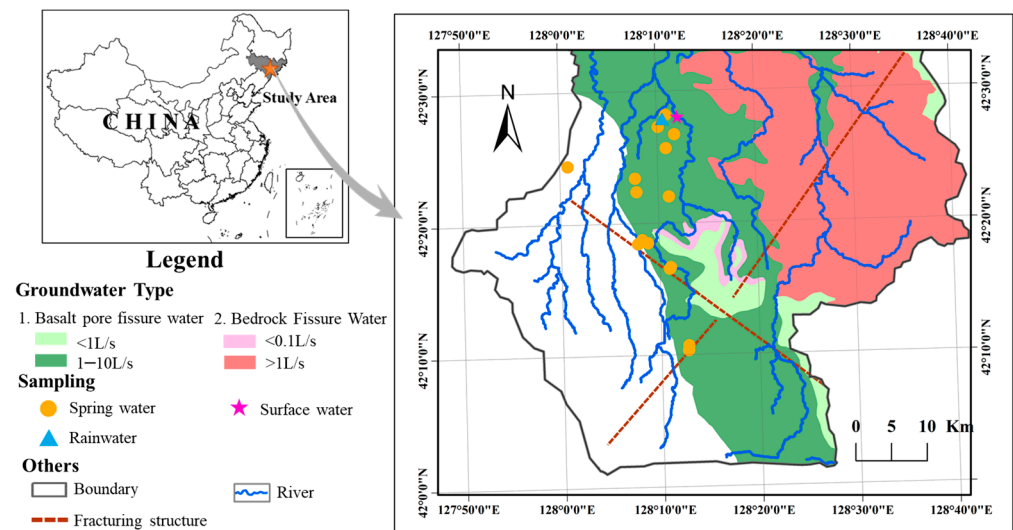


**Figure 2.** Hydrogeological map and sampling sites of the study area.

The chemical composition and stable isotopes ( $^{18}\text{O}$  and D) were measured at the Public Technology Service Center of the Northeast Institute of Geography and Agroecology, Chinese Academy of Sciences. The cations and  $\text{SO}_4^{2-}$  were measured using an inductively coupled plasma emission spectrometer (ICP-7500, Agilent Technologies Inc., Santa Clara, CA, USA), and the detection limit was less than  $10 \mu\text{g/L}$ . The other anions were measured by titration, and the detection limit was  $1 \text{ mg/L}$ . The detection accuracy was found to be 5%. Anion balance verification was conducted to ensure that the error range of credibility was  $\pm 10\%$ . Statistical Product Service Solutions (SPSS) was used for mathematical statistical analysis of each index of hydrochemistry data.

The hydrogen and oxygen isotopes were measured using a stable isotope mass spectrometer (MAT253, Thermo Finnigan Inc., San Jose, California, USA), and the determination accuracies of  $\delta\text{D}$  and  $\delta^{18}\text{O}$  were  $\pm 2\%$ . The results are reported as the per mil deviation relative to the VSMOW standard.

$$\delta = \left( \frac{R_{\text{Sample}} - R_{\text{VSMOW}}}{R_{\text{VSMOW}}} - 1 \right) \times 1000\text{‰} \quad (1)$$

where  $R_{\text{sample}}$  is the ratio of D/H or  $^{18}\text{O}/^{16}\text{O}$  in the water samples, and  $R_{\text{VSMOW}}$  is the ratio of D/H or  $^{18}\text{O}/^{16}\text{O}$  of the VSMOW standard.

### 2.3. Age of Water

Tritium was measured using an ultralow background liquid scintillation spectrometer (Quantulus 1220). The isotopic dating equation was as follows:

$$t = -\frac{T}{0.693} \ln \frac{N}{N_0} \quad (2)$$

where  $t$  is the isotopic age (a),  $N_0$  is the initial tritium concentration of the sample,  $N$  is the tritium concentration of the sample at time  $t$  (TU), and  $T$  is the half-life of tritium, namely, 12.43 a.

### 2.4. Water Interaction Elevation

Precipitation isotope has an elevation effect in precipitation isotopes. The groundwater recharge elevation of each sampling point in the study area can be calculated according to the  $\delta\text{D}$  and  $\delta^{18}\text{O}$  values. The calculation method is as follows:

$$H = (\delta_G - \delta_P) / K + h \quad (3)$$

where,  $H$  is the isotope infiltration height, m;  $h$  is the elevation of the sampling point, m;  $\delta_P$  is the value of  $\delta^{18}\text{O}$  (or  $\delta\text{D}$ ) of the atmospheric precipitation near the sampling point, dimensionless;  $\delta_G$  is the value of  $\delta^{18}\text{O}$  (or  $\delta\text{D}$ ) at the sampling point, dimensionless;  $K$  is the height gradient of atmospheric precipitation,  $-\delta/100$  m. The global average height gradient of  $\delta^{18}\text{O}$  is  $-0.25\text{‰}/100$  m.

### 2.5. Water Interaction Ratio

Stable oxygen isotope is selected as the tracer, and the two-terminal element mixed water source segmentation model is established according to the mass balance equation and concentration balance equation [18] to quantitatively analyze the contribution rate of rainwater and mineral water to river. The formula is as follows:

$$Q_R = Q_P + Q_G \quad (4)$$

$$\delta_R Q_R = \delta_P Q_P + \delta_G Q_G \quad (5)$$

where,  $Q_P$  and  $Q_G$  are the flow rates of surface water with rainwater and mineral water recharge;  $Q_R$  is the flow of surface water;  $\delta_P$ ,  $\delta_G$ , and  $\delta_R$  are the characteristic values of the  $^{18}\text{O}$  isotope of rainwater, mineral and surface water. By calculation, the recharge ratio of groundwater to surface water is  $K_{GR}$  as follows:

$$K_{GR} = \frac{Q_G}{Q_R} = \frac{(\delta_P - \delta_R)}{(\delta_P - \delta_G)} \quad (6)$$

The recharge ratio of atmospheric precipitation to surface water  $K_{PR}$  is:

$$K_{PR} = \frac{Q_P}{Q_R} = \frac{(\delta_R - \delta_G)}{(\delta_P - \delta_G)} \quad (7)$$

## 3. Results and Discussion

### 3.1. Hydrochemical Characteristics of Mineral Water

The statistical results calculated by SPSS 25.0 (Statistical Product Service Solutions, San Francisco, USA) present in Table 1 and Figure 3 pH value of mineral water ranged from 7.04 to 7.80, with an average value of 7.24, which was neutral. The coefficient of pH variation was 0.03, with minimal spatial variation. The content of cation components in  $\text{Na}^+ > \text{Ca}^{2+} > \text{Mg}^{2+} > \text{K}^+$ , and the concentration of anion is  $\text{HCO}_3^- \gg \text{SO}_4^{2-} > \text{Cl}^-$ . TDS concentration varied from 104.28 to 154.12 mg/L, with an average value of 123.08 mg/L, showing low mineralization. The content of metasilicate was within 35.02~57.69 mg/L, and the average value was 50.78 mg/L. All of samples reach the content requirements ( $\geq 25$  mg/L) of metasilicic acid type metasilicate mineral water in the limit index of "Drinking Natural Mineral Water" (GB8537-2008). They even belong to high metasilicate mineral water for drinking.

**Table 1.** Analytical results of stable hydrogen and oxygen isotope of water samples in study area.

Parameter	Unit	Min	Max	Mean	Sd	Cv
$\text{K}^+$	mg/L	1.56	3.30	2.63	0.49	0.19
$\text{Na}^+$	mg/L	4.91	10.44	7.94	1.85	0.23
$\text{Ca}^{2+}$	mg/L	4.99	12.20	7.07	2.23	0.31
$\text{Mg}^{2+}$	mg/L	2.22	5.41	3.95	0.94	0.24
$\text{HCO}_3^-$	mg/L	43.10	75.82	55.88	7.75	0.14
$\text{Cl}^-$	mg/L	0.55	3.35	1.82	0.97	0.54
$\text{SO}_4^{2-}$	mg/L	2.18	7.66	4.08	1.72	0.42
TDS	mg/L	104.28	154.12	123.08	12.26	0.10
$\text{H}_2\text{SiO}_3$	mg/L	35.02	57.69	50.78	6.50	0.13
pH	-	7.04	7.80	7.24	0.21	0.03

Note: Sd means standard deviation, Cv means coefficient of variation.

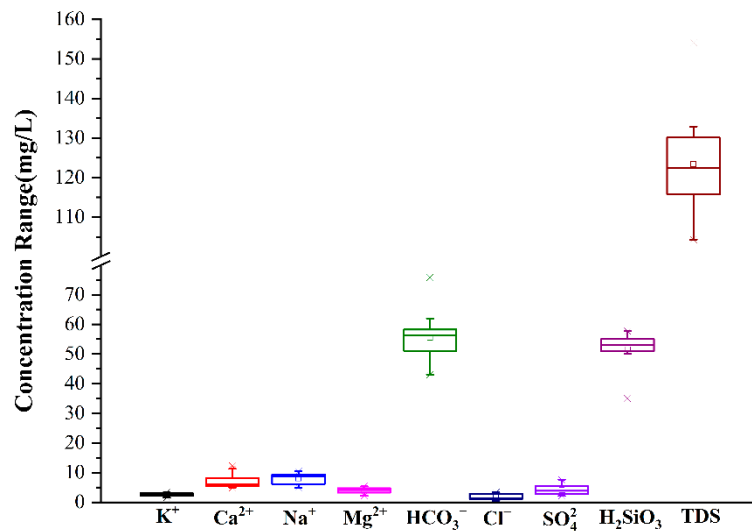


Figure 3. Box diagram of main components.

According to the metasilicate content of 15 mineral water samples, we drew the spatial distribution map of metasilicate content (Figure 4) using Surfer and the Kriging interpolation method.

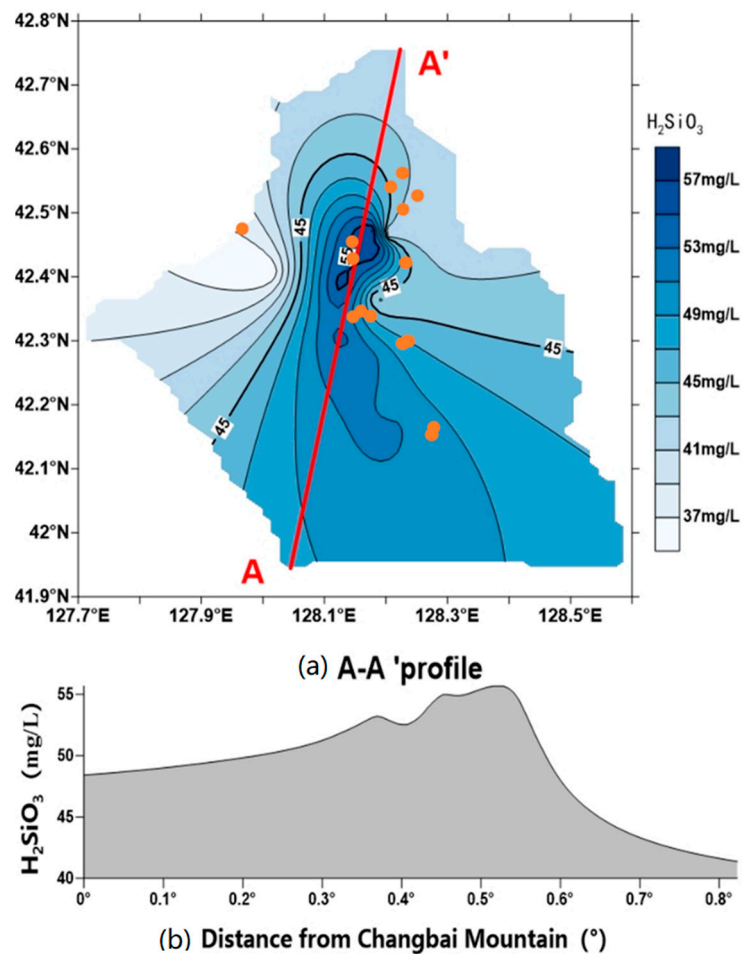


Figure 4. Spatial distribution of metasilicic acid in mineral water in the study area (the points present sampling sites).

Figure 4 exhibits the metasilicate content in study area was mainly distributed in 35–59 mg/L, and presented a trend of high center and low surrounding. We selected A-A' profile to study the relationship between metasilicate content and the distance from Changbai Mountain. At the A-A' profile, the content of metasilicate increased slowly first and then decreased sharply. What is the cause? In the southwest of the study area, Changbai Mountain has a high altitude, and the groundwater flows from south to north. The exposed strata are mainly Cenozoic volcanic rocks, and the basalt pore water is widely distributed in the region (Figure 2). The longer the distance from Changbai Mountain and the runoff time is, the more components were dissolved. The content of salt minerals is reduced, so the directly dissolved metasilicate is also reduced. However, the content of metasilicate in the northern region still over 35 mg/L, which is due to groundwater recharge with high metasilicate in the south.

The Piper and total ionic salinity (TIS) [41] diagrams were drawn (Figure 5a) to get hydrochemistry type of mineral water. TIS of waters ranges from 1.6 to 2.8 meq/L. Cations were mainly  $Ca^{2+}$  and  $Na^+$  In the anion,  $HCO_3^-$  took an absolute advantage, and its distribution as relatively concentrated. The Piper diagram classified hydrochemistry type into  $HCO_3$ -Ca-Na type water,  $HCO_3$ -Ca-Mg type, followed by  $HCO_3$ -Na-Mg-Ca type water,  $HCO_3$ -Na-Ca-Mg type.

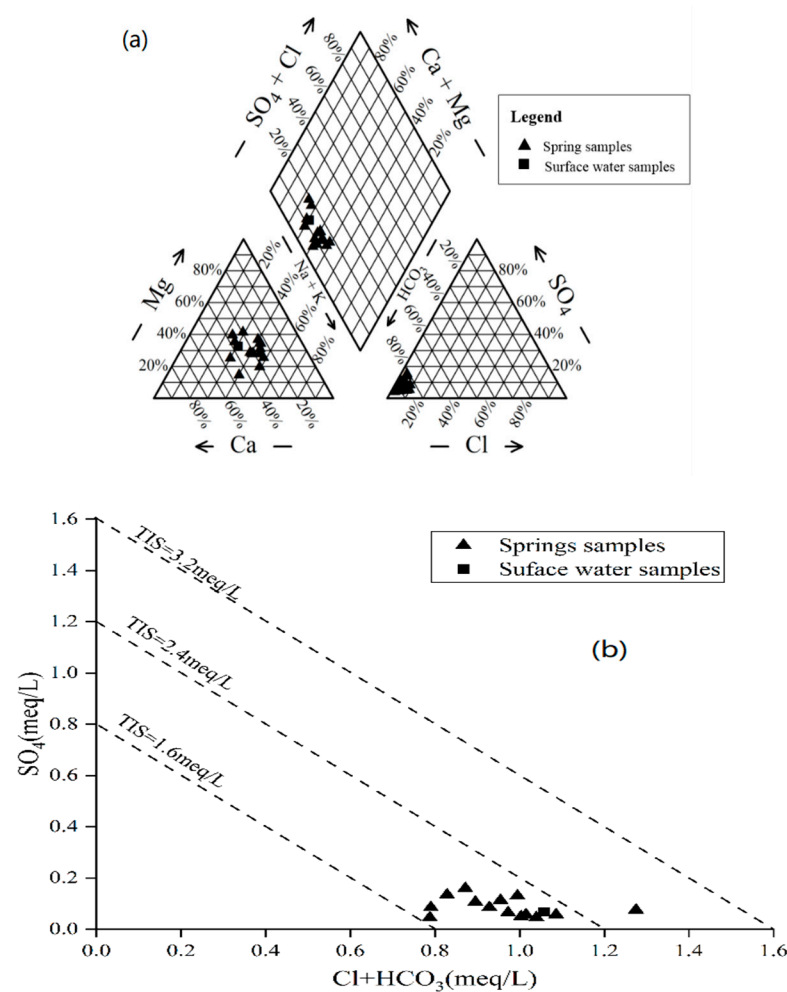


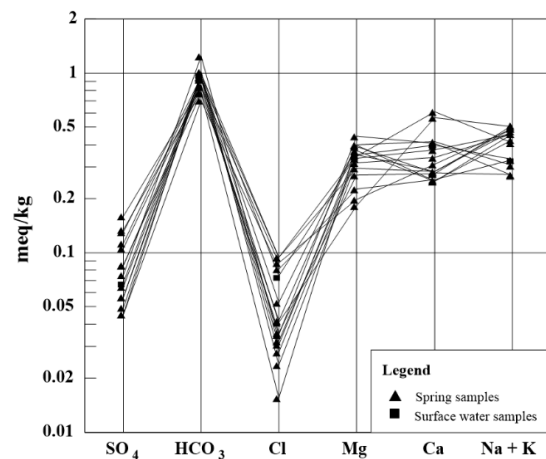
Figure 5. The piper diagram (a) and correlation diagram of  $SO_4$  vs.  $HCO_3 + Cl$  reporting the iso-salinity lines (b) of water samples.

Furthermore, the concentration of metasilicate in surface water was as high as 40.38 mg/L. The hydrochemistry type of surface water is very similar to mineral water, belonging to HCO<sub>3</sub>-Ca-Mg-Na type. It can be seen that the surface water and mineral water in this area have a relationship, and the mineral water may recharge surface water.

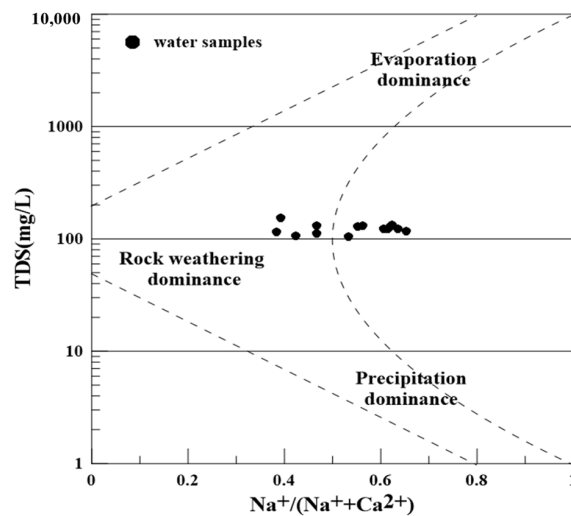
3.2. Formation Process of Solutes in Mineral Water

Schoeller diagram is a common method to study hydrochemistry characteristic. With a simple diagram, it can clearly analyze the concentration changes of main ions (Cl<sup>-</sup>, SO<sub>4</sub><sup>2-</sup>, HCO<sub>3</sub><sup>-</sup>, Na<sup>+</sup>, K<sup>+</sup>, Ca<sup>2+</sup>, Mg<sup>2+</sup>) in many samples [42]. The parallelism degree of the lines between different points reflects the differences in water supply and formation processes. In Figure 6, lines between different points are almost parallel, indicating that supply sources of mineral water are similar.

Gibbs' diagram can be used to identify the main factors controlling the evolution mechanism of chemical types of groundwater [43]. In Gibbs' model, the dominant process of groundwater formation is divided into three types: (1) precipitation, (2) rock weathering, and (3) evaporation mechanism. In study area, TDS concentration of mineral water was between 104.28 and 154.12 mg/L, with an average value of 123.08 mg/L. Na<sup>+</sup>/(Na<sup>+</sup> + Ca<sup>2+</sup>) was mainly between 0.3~0.7. It can be seen from Figure 6b,c that rock weathering in this area is dominant [44,45]. Silicate has a great influence on water bodies, which is the main factor controlling the origin of hydrochemistry [46].

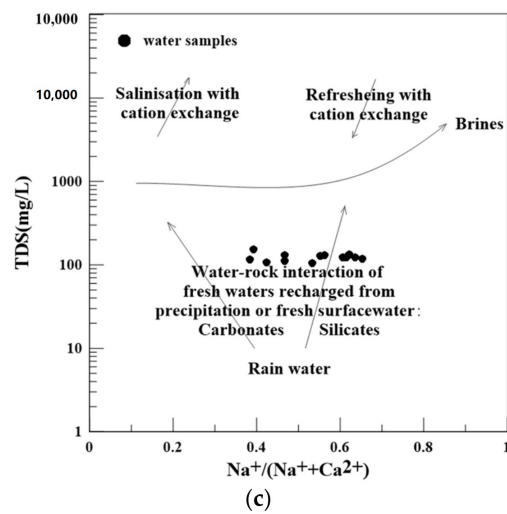


(a)



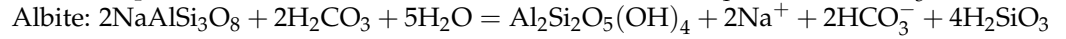
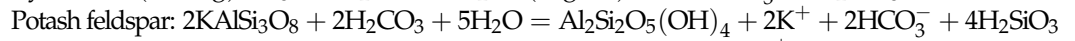
(b)

Figure 6. Cont.



**Figure 6.** Mineral water formation process: (a) Schoeller diagram, (b) Gibbs diagram, (c) modified Gibbs diagram.

The main aquifer media in study area is basalt, whose main components are feldspar, pyroxene, and olivine. The SI for the associated minerals in mineral water was calculated by PHREEQC (Table 2). All the minerals were unsaturated or SI is close to 0, indicating they had a tendency to dissolve [28]. Mineral water in the area was low-salinity with a large amount of CO<sub>2</sub>. The process of main water-rock reaction is as follows:



**Table 2.** SI values of mineral water samples for specific minerals.

Mineral Water Number	Potash Feldspar	Albite	Anorthite	Pyroxene
Average SI of mineral water	0.02	−1.83	−5.73	−5.61

In conclusion, the solute source of mineral water in the area is similar. The formation process is dominated by rock weathering, which is mainly formed by water-rock interaction of silicate mineral weathering. The main source of metasilicate is the hydrolytic reaction of silicate and aluminosilicate minerals in the process of precipitation infiltration and runoff.

### 3.3. Age of Mineral Water

Hydrological circulation of natural water leads to isotope fractionation and water mixing, resulting in different δD and δ<sup>18</sup>O contents. δD and δ<sup>18</sup>O values in groundwater are often used to trace the source, recharge area, and interactions with other water [47]. The variation range of δD and δ<sup>18</sup>O of the mineral water in study area is relatively small (Table 3). During the abundant water period, the variation range of δD was −100.53‰~−95.83‰, with an average of −98.59‰. The variation range of δ<sup>18</sup>O was −14.17‰~−13.36‰, with an average of −13.83‰. During the dry period, the variation range of δD was −102.45‰~−98.36‰, with an average value of −100.57‰. The variation range of δ<sup>18</sup>O was −14.95‰~−13.95‰, with an average value of −14.47‰. δD and δ<sup>18</sup>O of rainwater was −59.35‰ and −9.33‰. the surface values were −94.41‰ and −13.10‰ in abundant water period and −95.60‰ and −13.53‰ in dry period water. It can be seen that the hydrogen and oxygen isotopes of mineral and surface water in abundant water period (September 2019) are more abundant than those in dry water period (April 2019). This is

because the study area is located in the inland area with high latitude, the temperature and seasonal effect of the isotope is extremely obvious.

**Table 3.** Analytical results of stable hydrogen and oxygen isotope.

Water Types	Time & Quantity	$\delta D_{V-SMOW}/\text{‰}$			$\delta^{18}O_{V-SMOW}/\text{‰}$		
		Max	Min	Mean	Max	Min	Mean
Spring	April 2019	−98.36	−102.45	−100.57	−13.95	−14.95	−14.47
	September 2019	−95.83	−100.53	−98.59	−13.36	−14.17	−13.83
Surface water	April 2019	−95.60	−95.60	−95.60	−13.53	−13.53	−13.53
	September 2019	−94.41	−94.41	−94.41	−13.10	−13.10	−13.10
Precipitation	September 2019	−59.35	−59.35	−59.35	−9.33	−9.33	−9.33

Tritium concentration distribution ranged from 1.9 to 9.8 TU, with an average value of 6.1 TU. Mineral water is mainly supplied by “modern water”. The water age distribution ranged from 27.7–57.2 a, with an average of 35.5 a. Water age decreased with the increasing altitude of mineral water location (Table 3) It better confirms the previous law of spatial distribution of metasilicate content (Figure 4). Water age affects the residence time, thus has an influence on water-rock interaction time. Therefore, when the altitude is high, the distance from Changbai Mountain is short, which reduces water-rock interaction time and decreases metasilicate content.

### 3.4. Interaction of Mineral and Surface Water

The interaction relationship between different water bodies can be clarified by analyzing the hydrogen and oxygen isotope components [48]. According to Wang Fengsheng’s study [49], the Local Meteoric Water Line (LMWL) in Changbai Mountain area is  $\delta D = 7.7\delta^{18}O + 9.11$ , which is not different from the Global Meteoric Water Line (GMWL)  $\delta D = 8\delta^{18}O + 10$ , indicating that the local evaporation is not strong [49].

In September, water samples in study area were all located between GMWL and LMWL (Figure 7), indicating that the main source of mineral water is precipitation. In April, the  $\delta D$  and  $\delta^{18}O$  values of water samples slightly deviated from the LMWL. Some fell on the GMWL and LMWL, but most of them fell on the upper left of two lines. The slopes of  $\delta D$  and  $\delta^{18}O$  line were smaller than GMWL and LMWL, indicating that the mineral spring in the area was supplied by rainwater, but also by the infiltration of certain condensate [50–52].

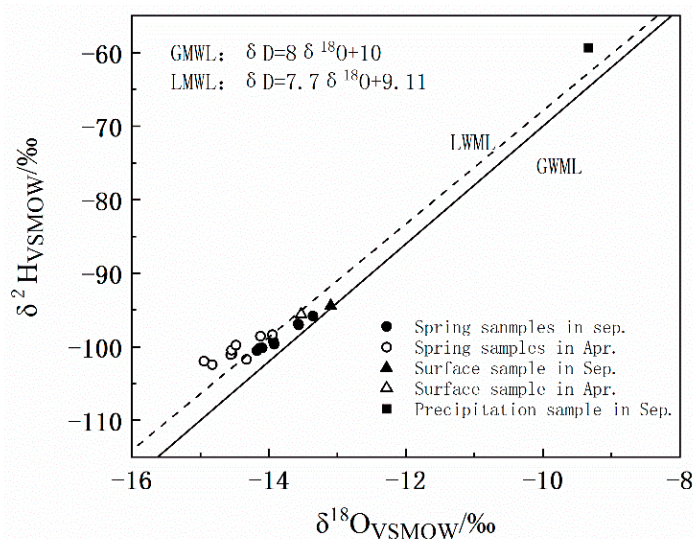


**Figure 7.**  $\delta D$ – $\delta^{18}O$  Plot of water samples.

The results of recharge elevation are shown in Table 4. The basalt pore water in the region is mainly recharged by meteoric precipitation and condensate infiltration, and the replenishment elevation is much higher than elevation of mineral water. The replenishment area is mainly located in the nature reserve which is on the north side of Tianchi lake in the south. After the meteoric precipitation and condensation water infiltrate into the groundwater, water accumulates in the basalt pore. Under the influence of topography, part of the basalt pore water flows from south to north, and the main runoff channel is in Junjianshan basalt. After the basalt pore water runoff enters the study area, it overflows the surface in the way of spring or spring group in areas such as low-lying valleys. From the above analysis, it can be proved that atmospheric precipitation is the main recharge source of surface and mineral water in study area. Meanwhile, mineral water is distributed around rivers and the metasilicate content of surface water is 40.38 mg/L, which is close to mineral water. The content of stable isotope and  $Cl^-$  have a similar tendency (Figure 8). These indicate that there is interaction between mineral and surface water. According to Formulas (4)–(7), the ratio of mineral water recharging surface water is 83.7%, which is relatively high. That proved the importance of mineral water to water resources of the whole basin in study area.

**Table 4.** Analytical results of tritium of groundwater in study area.

Water Types	Sampling Height/m	Recharge Height/m	Tritium Concentration/TU	Age/a
Mineral water	663	1801	1.9	57.2
	693	1835	5.4	38.4
	712	1824	8.2	30.9
	1143	2393	9.8	27.7
	956	1855	9.2	28.9
	925	1893	7.4	32.8
	812	2110	5.6	37.8
712	1824	6.1	36.2	
Surface water	666	1398	8.7	29.9

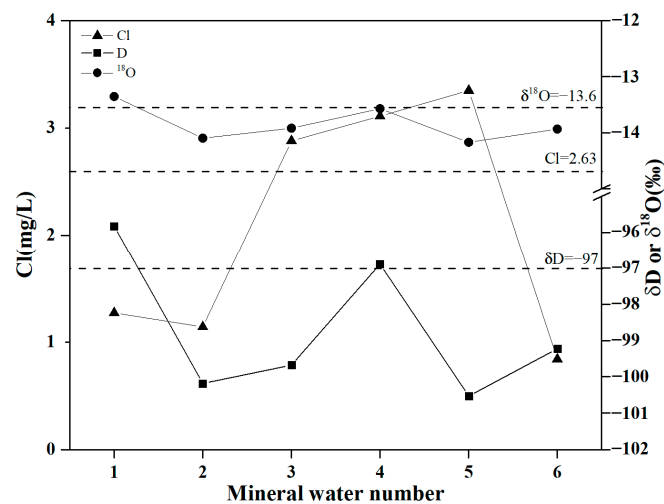


**Figure 8.**  $\delta D$ ,  $\delta^{18}O$  and  $Cl^-$  content of mineral and surface water (the dash lines present content of surface water).

#### 4. Conclusions

A combined application of hydrochemistry and stable oxygen and hydrogen isotope method is performed to investigate the mineral water in the Changbai Mountain area. The main conclusions are as follows.

(1) The hydrochemistry types of natural mineral water in Changbai Mountain area are mainly  $HCO_3-Ca-Na$  type and  $HCO_3-Ca-Mg$  type. The average content of metasilicate is

50.78 mg/L, which is a high-quality mineral water. The age distribution range of mineral water is 27.7–57.2 a, with an average of 35.5 a. The concentration of metasilicate is closely related to mineral water retention time and runoff length. And (2) the hydrochemistry formation process and supply source of mineral water is similar. The formation process is dominated by the mechanism of rock weathering, which is mainly formed by water-rock interaction of silicate mineral. The main source of metasilicate is the hydrolytic reaction of pyroxene and olivine in the process of precipitation and runoff under acidic conditions.

(3) Atmospheric precipitation is the main recharge source of mineral and surface water in this area. At the same time, surface water is closely linked to mineral water in the valley area, the water level is low and mineral water recharges the surface water. The recharge ratio of atmospheric precipitation to surface water is 16.3%, while the recharge ratio of groundwater to surface water is as high as 83.7%, so the river water sample also has a high content of metasilicate.

**Author Contributions:** Project administration, J.B.; methodology, formal analysis, writing—original draft, Y.L.; writing—review and editing, Y.M.; data curation, visualization, J.L.; visualization, Y.Y.; data curation, W.S. All authors have read and agreed to the published version of the manuscript.

**Funding:** This work was supported by the Key Projects of Jilin Provincial Department of Science and Technology (grant number 20190303076SF) and the National Key R&D Program of China (grant number 2019YFC0409103).

**Institutional Review Board Statement:** Not applicable.

**Informed Consent Statement:** Not applicable.

**Data Availability Statement:** The processed data required to reproduce these findings cannot be shared at this time as the data also forms part of an ongoing study.

**Conflicts of Interest:** The authors declare no conflict of interest.

## References

1. Medici, G.; Bajak, P.; West, L.J.; Chapman, P.J.; Banwart, S.A. DOC and nitrate fluxes from farmland; impact on a dolostone aquifer KCZ. *J. Hydrol.* **2021**, *595*, 125658. [[CrossRef](#)]
2. Qin, C.; Li, S.L.; Waldron, S.; Yue, F.J.; Wang, Z.J.; Zhong, J.; Ding, H.; Liu, C.Q. High-frequency monitoring reveals how hydrochemistry and dissolved carbon respond to rainstorms at a karstic critical zone, Southwestern China. *Sci. Total Environ.* **2020**, *714*, 136833. [[CrossRef](#)] [[PubMed](#)]
3. Appelo, C.A.J.; Postma, D. Geochemistry, groundwater and pollution. In *Balkema*; CRC Press: Boca Raton, FL, USA, 2005.
4. Fuoco, I.; de Rosa, R.; Barca, D.; Figoli, A.; Gabriele, B.; Apollaro, C. Arsenic polluted waters: Application of geochemical modelling as a tool to understand the release and fate of the pollutant in crystalline aquifers. *J. Environ. Manag.* **2022**, *301*, 113796. [[CrossRef](#)]
5. Fuoco, I.; Marini, L.; de Rosa, R.; Figoli, A.; Gabriele, B.; Apollaro, C. Use of reaction path modelling to investigate the evolution of water chemistry in shallow to deep crystalline aquifers with a special focus on fluoride. *Sci. Total Environ.* **2022**, *830*, 154566. [[CrossRef](#)] [[PubMed](#)]
6. Kløve, B.; Ala-aho, P.; Bertrand, G.; Boukalova, Z.; Ertürk, A.; Goldscheider, N.; Ilmonen, J.; Karakaya, N.; Kupfersberger, H.; Kværner, J.; et al. Groundwater dependent ecosystems. Part I: Hydroecological status and trends. *Environ. Sci. Policy* **2011**, *7*, 770–781. [[CrossRef](#)]
7. Shi, X.D.; Kang, X.B.; Xu, M.; Deng, H.K. Hydrochemical characteristics and evolution laws of karst groundwater in the slope zone of the canyon area, Sichuan-Yunnan Plateau. *Acta Geol. Sin.* **2019**, *93*, 2975–2984.
8. Amiri, V.; Kamrani, S.; Ahmad, A.; Bhattacharya, P.; Mansoori, J. Groundwater quality evaluation using Shannon information theory and human health risk assessment in Yazd province, central plateau of Iran. *Environ. Sci. Pollut. Res.* **2021**, *28*, 1108–1130.
9. Tang, C.L.; Zheng, X.Q.; Liang, Y.P. Hydrochemical Characteristics and Formation Causes of Ground Karst Water Systems in Longzici Spring Catchment. *Environ. Sci.* **2020**, *41*, 2087–2209.
10. Xiong, G.Y.; Fu, T.F.; Han, J.B.; Chen, G.Q.; Xu, X.Y.; Xu, X.L.; Liu, G.Q.; Liu, W.Q. Hydrogeochemical and Isotopic Characteristics of Groundwater in Dagu River Basin. *Adv. Mar. Sci.* **2019**, *37*, 626–637.
11. Amiri, V.; Li, P.; Bhattacharya, P.; Nakhaei, M. Mercury pollution in the coastal Urmia aquifer in northwestern Iran: Potential sources, mobility, and toxicity. *Environ. Sci. Pollut. Res.* **2021**, *28*, 17546–17562. [[CrossRef](#)]
12. He, J.; Zhang, Y.K.; Zhao, Y.Q.; Han, S.B.; Liu, Y.Q.; Zhang, T. Hydrochemical Characteristics and Possible Controls of Groundwater in the Xialatuo Basin Section of the Xianshui River. *Environ. Sci.* **2019**, *40*, 1236–1244.

13. Wei, X.; Zhou, J.L.; Nai, W.H.; Zeng, Y.Y.; Fan, W.; Li, B. Hydrochemical Characteristics and Evolution of Groundwater in the Kashgar Delta Area in Xinjiang. *Environ. Sci.* **2019**, *40*, 4042–4051.
14. Sohrabi, N.; Kalantari, N.; Amiri, V.; Saha, N.; Berndtsson, R.; Bhattacharya, P.; Ahmad, A. A probabilistic-deterministic analysis of human health risk related to the exposure to potentially toxic elements in groundwater of Urmia coastal aquifer (NW of Iran) with a special focus on arsenic speciation and temporal variation. *Stoch. Environ. Res. Risk Assess.* **2020**, *35*, 1509–1528. [[CrossRef](#)]
15. Getnet, T.B.; Zelalem, L.A.; Alebachew, T.K.; Mohammed, S.M.; Gashaw, W. Hydrogeochemical and isotopic signatures of groundwater in the Andasa watershed, Upper Blue Nile basin, Northwestern Ethiopia. *J. Afr. Earth Sci.* **2019**, *160*, 103617.
16. Locsey, K.L.; Grigorescu, M.; Cox, M.E. Water–Rock interactions: An investigation of the relationships between mineralogy and groundwater composition and flow in a subtropical basalt aquifer. *Aquat. Geochem.* **2012**, *1*, 45–75. [[CrossRef](#)]
17. Vaughn, B.H.; Fountain, A.G. Stable isotopes and electrical conductivity as keys to understanding water pathways and storage in South Cascade Glacier, Washington, USA. *Ann. Glaciol.* **2005**, *40*, 107–112. [[CrossRef](#)]
18. Wang, Y.S.; Cheng, X.X.; Zhang, M.N.; Qi, X.F. Hydrochemical characteristics and formation mechanisms of Malian River in Yellow River basin during dry season. *Environ. Chem.* **2018**, *37*, 164–172.
19. Liu, S.T.; Zhang, D.; Li, Y.H.; Yang, J.M.; Zhou, S.; Wang, Y.T.; Huang, X.Y.; Zhang, Z.Y.; Yang, W.; Jia, B.J. Water Sources and Factors Controlling on Hydro-chemical Compositions in the Yiluo River Basin. *Environ. Sci.* **2020**, *41*, 1184–1196.
20. Zhang, Y.; Su, C.L.; Ma, Y.H.; Liu, W.J. Indicators of Groundwater Evolution Processes Based on Hydrochemistry and Environmental Isotopes: A Case Study of the Dongyuan Drinking Water Source Area in Ji'nan City. *Environ. Sci.* **2019**, *40*, 2667–2674.
21. Su, X.S.; Gao, R.M.; Yuan, W.Z.; Lu, S.; Su, D.; Zhang, L.H.; Meng, X.F.; Zuo, E.D. Research on River Recharge Based on Environmental Isotope Technology: A Case Study of Huangjia Riverside Well Field in Shenyang City. *J. Jilin Univ. (Earth Sci. Ed.)* **2019**, *49*, 763–773.
22. Han, J.B.; Xu, J.X.; Xu, K.; Zhong, Y.; Qin, X.W.; Ma, H.Z. The exchange relationship of surface water-groundwater and uranium flux in the Gas Hure Salt Lake of northwest Qaidam Basin, China. *J. Lake Sci.* **2019**, *31*, 1738–1748.
23. Kong, X.L.; Wang, S.Q.; Ding, F.; Liang, Y.H. Source of Nitrate in Surface Water and Shallow Groundwater Around Baiyangdian Lake Area Based on Hydrochemical and Stable Isotopes. *Environ. Sci.* **2018**, *39*, 2624–2631.
24. Wen, G.C.; Wang, W.K.; Duan, L.; Gu, X.F.; Li, Y.M.; Zhao, J.H. Quantitatively evaluating exchanging relationship between river water and groundwater in Bayin River Basin of northwest China using hydrochemistry and stable isotope. *Arid Land Geogr.* **2018**, *41*, 734–743.
25. Sun, C.J.; Chen, W. Relationship between Groundwater and Surface Water Based on Environmental Isotope and Hydrochemistry in Upperstream of the Haihe River Basin. *Sci. Geogr. Sin.* **2018**, *38*, 790–799.
26. Zhao, H.; Meng, Y.; Dong, W.H.; Lv, Y.; Wu, X.C. Hydrochemistry and Stable Isotopes Characteristics of Water within Naoli River Basin. *Yellow River* **2017**, *39*, 73–78.
27. Yan, B.Z.; Xiao, C.L.; Liang, X.J.; Wei, R.C.; Wu, S.L. Characteristics and genesis of mineral water from Changbai Mountain, Northeast China. *Environ. Earth Sci.* **2015**, *7*, 4819–4829. [[CrossRef](#)]
28. Yan, B.Z.; Xiao, C.L.; Liang, X.J.; Wu, S.L. Hydrogeochemical tracing of mineral water in Jingyu County, Northeast China. *Environ. Geochem. Health* **2016**, *38*, 291–307. [[CrossRef](#)]
29. Liang, X.J.; Tian, H.; Xiao, C.L.; Li, M.Q.; Sun, Y.; Li, Y.X. Recharge of natural mineral water Jingyu County, northeastern China. *E3S Web Conf.* **2019**, *98*, 1032. [[CrossRef](#)]
30. Xiao, C.L.; Yuan, Y.J.; Liang, X.J.; Yang, W.F.; Sun, Y. Sources of metasilicate in mineral water of Jingyu County, northeastern China. *E3S Web Conf.* **2019**, *98*, 1052. [[CrossRef](#)]
31. Liang, X.J.; Li, S.; Li, Y.X.; Wu, S.L.; Xiao, R.; Xiao, C.L. Experimental study of evolution of aqueous SiO<sub>2</sub> in the mineral water in basalt beds of Jingyu County, China. *Procedia Earth Planet. Sci.* **2013**, *7*, 500–503.
32. Yan, B.Z.; Xiao, C.L.; Liang, X.J.; Wu, S.L. Influences of pH and CO<sub>2</sub> on the formation of Metasilicate mineral water in Changbai Mountain, Northeast China. *Appl. Water Sci.* **2017**, *7*, 1657–1667. [[CrossRef](#)]
33. Zhang, Q.; Liang, X.J.; Xiao, C.L. The Hydrogeochemical Characteristic of Mineral Water Associated with Water-rock Interaction in Jingyu County, China. *Procedia Earth Planet. Sci.* **2017**, *17*, 726–729. [[CrossRef](#)]
34. Liu, T. Study on the Sustainable Use of Natural Spring Water in the Basalt Area of Jingyu County. Master's Thesis, Jilin University, Changchun, China, 2015.
35. Lin, L. The Research on the Genesis and the Exploitation Control Scheme of the Mineral Spring Water Resource in the Changbai Mountain District. Master's Thesis, Jilin University, Changchun, China, 2016.
36. Gao, Y. Research on the Recharge Conditions and Formation Mechanism of Mineral Water in Fusong County. Master's Thesis, Jilin University, Changchun, China, 2016.
37. Zhang, Z.Z. Study on the Carrying Capacity and Sustainable Utilization of Water Resources in Fusong County. Master's Thesis, Jilin University, Changchun, China, 2016.
38. Tao, Y. Study on the Division of Natural Mineral Drinking Water Source Protection Areas in Fusong of Changbai Mountain in Jilin Province. Master's Thesis, Jilin University, Changchun, China, 2013.
39. Gao, Y.; Bian, J.M.; Song, C.; Cong, L. Response of Mineral Water Resources to Precipitation Change Based on Wavelet Analysis in Fusong County. *J. China Hydrol.* **2016**, *36*, 35–40.

40. Ma, Y.X.; Bian, J.M.; Sun, X.Q.; Wu, J.J. Hydrochemical Characteristics and Health Evaluation of Natural Mineral Water in Fusong County, Jilin Province. *J. Jilin Agric. Univ. (China)*. Available online: <https://kns.cnki.net/kcms/detail/detail.aspxdbcode=CAPJ&dbname=CAPJLAST&filename=JLNY20190704001&v=tErk7cedzEIKukTN5Mc6E76dKr-mQw7rw29E%25mmd2B6wkRKdE4R8cak3OAKxnq11Sfzep> (accessed on 8 July 2019).
41. Apollaro, C.; di Curzio, D.; Fuoco, I.; Buccianti, A.; Dinelli, E.; Vespasiano, G.; Castrignano, A.; Rusi, S.; Barca, D.; Figoli, A.; et al. A multivariate non-parametric approach for estimating probability of exceeding the local natural background level of arsenic in the aquifers of Calabria region (Southern Italy). *Sci. Total Environ.* **2022**, *806*, 150345. [[CrossRef](#)]
42. Aksever, F. Hydrogeochemical characterization and water quality assessment of springs in the Emirdağ (Afyonkarahisar) basin, Turkey. *Arab. J. Geosci.* **2019**, *12*, 780. [[CrossRef](#)]
43. Marandi, A.; Shand, P. Groundwater chemistry and the Gibbs Diagram. *Appl. Geochem.* **2018**, *97*, 209–212. [[CrossRef](#)]
44. Amiri, V.; Bhattacharya, P.; Nakhaei, M. The hydrogeochemical evaluation of groundwater resources and their suitability for agricultural and industrial uses in an arid area of Iran. *Groundw. Sustain. Dev.* **2021**, *12*, 100527. [[CrossRef](#)]
45. Sohrabi, N.; Kalantari, N.; Amiri, V.; Nakhaei, M. Assessing the chemical behavior and spatial distribution of yttrium and rare earth elements (YREEs) in a coastal aquifer adjacent to the Urmia Hypersaline Lake, NW Iran. *Environ. Sci. Pollut. Res.* **2017**, *24*, 20502–20520. [[CrossRef](#)]
46. Amiri, V.; Berndtsson, R. Fluoride occurrence and human health risk from groundwater use at the west coast of Urmia Lake, Iran. *Arab. J. Geosci.* **2020**, *13*, 921. [[CrossRef](#)]
47. Zhang, W.Q.; Wang, W.F.; Liu, S.Q.; Chen, J.S. Relationship of recharge runoff and drainage for the mineral water in the Changbai Mountain. *J. Hohai Univ. (Nat. Sci.)* **2019**, *47*, 108–113.
48. Sun, X.Q.; Bian, J.M.; Zhang, C.P.; Wang, Y.; Wan, H.L.; Jia, Z. Hydrochemistry Characteristics and Water Quality Assessment for Irrigation along the Second Songhua River in the South of the Songnen Plain, Northeast China. *Pol. J. Environ. Stud.* **2020**, *29*, 371–395.
49. Wang, F.S. The law of O and Histopic Concentration Field on the Time-space Distribution and Environmental Effect of Atmospheric Water in Jilin Province. *Jilin Geol.* **1997**, *16*, 52–57.
50. Amiri, V.; Nakhaei, M.; Lak, R.; Kholghi, M. Geophysical, isotopic, and hydrogeochemical tools to identify potential impacts on coastal groundwater resources from Urmia hypersaline Lake, NW Iran. *Environ. Sci. Pollut. Res.* **2016**, *23*, 16738–16760. [[CrossRef](#)] [[PubMed](#)]
51. Amiri, V.; Nakhaei, M.; Lak, R. Using radon-222 and radium-226 isotopes to deduce the functioning of a coastal aquifer adjacent to a hypersaline lake in NW Iran. *J. Asian Earth Sci.* **2017**, *147*, 128–147. [[CrossRef](#)]
52. Li, Y.H.; Bian, J.M.; Li, J.L.; Ma, Y.X.; Aaguiano, J.H.H. Hydrochemistry and stable isotope indication of natural mineral water in Changbai Mountain, China. *J. Hydrol. Reg. Stud.* **2022**, *40*, 101047. [[CrossRef](#)]